Title

CRM1 Inhibition Promotes Cytotoxicity in Ewing Sarcoma Cells by Repressing EWS-FLI1–Dependent IGF-1 Signaling

Authors

Sun, Haibo
Lin, De-Chen
Cao, Qi
et al.

Peer reviewed

CRM1 Inhibition Promotes Cytotoxicity in Ewing Sarcoma Cells by Repressing EWS-FLI1– Dependent IGF-1 Signaling

Haibo Sun[1,2], De-Chen Lin[2,3], Qi Cao[2], Xiao Guo[2], Helene Marijon[2], Zhiqiang Zhao[4], Sigal Gery[2], Liang Xu[3], Henry Yang[3], Brendan Pang[5], Victor Kwan Min Lee[5], Huey Jin Lim[5], Ngan Doan[6], Jonathan W. Said[6], Peiguo Chu[7], Anand Mayakonda[3], Tom Thomas[2], Charles Forscher[2], Erkan Baloglu[8], Sharon Shacham[8], Raja Rajalingam[1], and H. Phillip Koeffler[2,3,9]

Abstract

Ewing sarcoma (EWS) is an aggressive bone malignancy that mainly affects children and young adults. The mechanisms by which EWS (EWSR1) fusion genes drive the disease are not fully understood. CRM1 (XPO1) traffics proteins from the nucleus, including tumor suppressors and growth factors, and is over-expressed in many cancers. A small-molecule inhibitor of CRM1, KPT-330, has shown therapeutic promise, but has yet to be investigated in the context of EWS. In this study, we demonstrate that CRM1 is also highly expressed in EWS. shRNA-mediated or pharmacologic inhibition of CRM1 in EWS cells dramatically decreased cell growth while inducing apoptosis, cell-cycle arrest, and protein expression alterations to several cancer-related factors. Interestingly, silencing of CRM1 markedly reduced EWS–

FLI1 fusion protein expression at the posttranscriptional level and upregulated the expression of the well-established EWS-FLI1 target gene, insulin-like growth factor binding protein 3 (IGFBP3), which inhibits IGF-1. Accordingly, KPT-330 treatment attenuated IGF-1–induced activation of the IGF-1R/AKT pathway. Furthermore, knockdown of IGFBP3 increased cell growth and rescued the inhibitory effects on IGF-1 signaling triggered by CRM1 inhibition. Finally, treatment of EWS cells with a combination of KPT-330 and the IGF-1R inhibitor, linsitinib, synergistically decreased cell proliferation both *in vitro* and *in vivo*. Taken together, these findings provide a strong rationale for investigating the efficacy of combinatorial inhibition of CRM1 and IGF-1R for the treatment of EWS. *Cancer Res; 76(9); 2687–97. ©2016 AACR.*

Introduction

Ewing sarcoma (EWS) is one of the most common and aggressive bone malignancies in children and young adults. Surgery and chemotherapy either with or without radiotherapy can cure 70% of patients, but those with metastatic disease are usually refractory (1, 2). Therefore, a compelling need exists for

[1]Immunogenetics and Transplantation Laboratory, Department of Surgery, University of California San Francisco, San Francisco, California. [2]Department of Medicine, Cedars-Sinai Medical Center, Los Angeles, California. [3]Cancer Science Institute of Singapore, National University of Singapore, Singapore. [4]Department of Musculoskeletal Oncology, The First Affiliated Hospital of Sun Yat-Sen University, Guangzhou, China. [5]Department of Pathology, National University Hospital Singapore, Singapore. [6]Department of Pathology and Laboratory Medicine, UCLA School of Medicine, Los Angeles, California. [7]Department of Pathology, City of Hope National Medical Center, Los Angeles, California. [8]Karyopharm Therapeutics Inc, Newton, Massachusetts. [9]National University Cancer Institute, National University Hospital Singapore, Singapore.

the development of more innovative and effective therapies. EWS is characterized by chromosomal translocations that fuse the *EWS* gene to an E26 transformation-specific transcription factor, most commonly *FLI1* (3). This major driver event is accompanied by few additional mutations, highlighting the importance of the EWS fusion protein in this disease (3–7). EWS-FLI1 acts as an oncogenic transcriptional factor, which enhances the survival and growth of EWS cells (8) through either activating or repressing thousands of genes (8, 9). CRM-1 (also known as XPO1) is a major nuclear export protein responsible for trafficking hundreds of proteins and RNAs out of the nucleus (10). CRM-1 cargos include many tumor-suppressor and growth-stimulating proteins, such as p53, p73, p21^{cip1}, p27^{kip1}, STAT3, FOXO, APC, BRCA1, survivin, and IκB (11, 12). CRM1 is upregulated in several types of cancer, and its overexpression correlates with a poor prognosis (11, 13–17). Importantly, CRM1 inhibition by the potent small-molecule selective inhibitor of nuclear export (SINE), KPT-330, has been suggested as a promising therapeutic option for a number of cancer types (18–23). In this study, we characterized the biologic significance of CRM1 in the context of EWS and determined the therapeutic merit of CRM1 inhibition for this malignancy.

Materials and Methods

Reagents and antibodies

The following reagents and antibodies were used in the current study: KPT-330 (Karyopharm Therapeutics Inc.); crizotinib and

linsitinib (MedKoo Sciences); human IGF-1, HGF, FLT-3L, IL3, IL6, SCF, and TPO (PROSPEC); actinomycin D, cycloheximide, and antibody against β-actin (Sigma-Aldrich); antibodies against p21^{cip1} (#2946), p-AKT (#4060), BAK (#12105), BAX (#5023), BIM (#2933), PUMA (#12450), p-BAD (#5284), p-MET (#3077), Met (#8198), DDIT3 (#L36F7), FOXO1 (C29H4), and p-MTOR (2971; Cell Signaling Technology); CRM1 (H300), FLI-1 (C19), Histone H3 (FL-136), GAPDH (FL-235), BCL-2 (100), BCL-XL (H-5), IGFBP3 (4), cyclin A1 (H230), cyclin D1 (A-12), c-MYC (C-19), p27^{kip1} (C-19), BCL-XL (H-5), BAX (N-20), PUMA (H-136), p53 (FL-393), AKT(5C10), IGF1-R1 (3B7), p-JNK (G-7), p-IGF1-R (Tyr1161), GAPDH (6C5), and MDM2 (SMP14; Santa Cruz Biotechnologies); BioT transfection reagent (Bioland Scientific); Flag-hCRM1 plasmid (Addgene); IGFBP3 siRNA lentiviral plasmid (i010368) and EWS-FLI siRNAs (ABM Inc.); Matrigel anti-rabbit IgG and anti-mouse conjugated HRP antibodies (BD Biosciences). siRNA pools targeting DDIT3 and p53 were purchased from Dharmacon. Bone marrow cells from normal donors were purchased from AllCells.

Cell culture, drug treatment, and cell viability assays

EWS cell lines were kindly provided by Dr. Kimberly Stegmaier (Harvard Medical School, Boston, MA) and Dr. Stephen L. Lessnick (University of Utah, Salt Lake City, UT), and were grown in DMEM (Corning) supplemented with 10% FBS, penicillin, and streptomycin. RH5 and MLS402 cell line were kindly provided by Dr. Javed Khan (National Institutes of Health, Bethesda, MD) and Dr. Pierre Åman (University of Gothenburg, Gothenburg, Sweden), respectively. The identity of all cell lines was recently verified by short tandem repeat analysis. Cell viability assays and analysis of drug synergy were performed as previously described (18). The extent of interaction between two drugs was presented using the combination index (CI; ref. 24).

Apoptosis and cell-cycle assays

Cells were seeded at 50% confluency in 6-well plates, and after overnight incubation, culture media were replaced with fresh media containing either diluent control or indicated drugs. After 24-hour incubation, cells were washed with PBS and stained with both propidium iodide (PI) and Annexin V (BD Biosciences), and assayed on a LSRII flow cytometer (BD Biosciences). Cell-cycle analysis was performed by PI staining (Sigma-Aldrich) for DNA content and followed by flow cytometric analysis. All flow cytometry data were analyzed using FlowJo software (Tree Star).

Immunoblotting and immunohistochemistry

Protein lysates from cells were extracted using ProteoJET Mammalian Cell Lysis Reagent (Thermo Scientific), and protein concentrations were determined by BCA assay (Thermo Scientific). Protein lysates were resolved by SDS-PAGE, transferred to PVDF membrane (Merck Millipore), and followed by immunoblotting procedures as previously described (18). To prepare nuclear and cytoplasmic fractions, cells were lysed in 10 mmol/L HEPES (pH 7.9), 10 mmol/L KCL, 0.1 mmol/L EDTA, 0.6% NP-40, 1 mmol/L DTT, and protease inhibitors (Thermo Scientific) and centrifuged at 16,000 g for 10 minutes to collect the soluble fraction (cytosolic extract). Insoluble pellets were lysed with the lysis buffer [20 mmol/L HEPES (pH 7.9), 0.4 mol/L NaCl, 1 mmol/L EDTA, 0.6% NP-40, 1 mmol/L DTT, and protease inhibitors] and centrifuged at 16,000 g for 10 minutes to collect the nuclear extracts. The nuclear and cytoplasmic fractions were then subjected to immunoblotting analysis. The immunohistochemistry was performed with standard procedures as previously described (18). CRM1 expression was scored using the H-score method as previously described (25).

Lentiviral infections

The target sequence of shCRM1 in pLKO.1 lentiviral vector is 5′-GCTCAAGAAGTACTGACACAT-3′. Cells were transduced with viral particles in the presence of 8 μg/mL polybrene for 16 hours followed by replacement of the lentivirus-containing media with fresh media. Two days after infection, puromycin (2 μg/mL) was added for 3 days to eliminate uninfected cells.

PCR

Total RNA was extracted using the RNeasy isolation Kit (Qiagen). For quantitative real-time PCR (qRT-PCR), cDNA was generated using the qScript cDNA Synthesis Kit (Quanta Biosciences). qRT-PCR was performed on CFX96 qPCR System (Biorad Inc). Expression of each gene was normalized to *GAPDH* as a reference. Primers for qRT-PCR are listed in Supplementary Table S1.

Animal models

All animal studies were approved by the Cedars-Sinai Institutional Animal Care and Use Committee. Seven-week-old female athymic nude mice [Crl:NU(NCr)-Foxn1^{nu}] were purchased from Charles River Laboratories and inoculated subcutaneously in both flanks with a suspension of EW8 or TC32 cells (2.0×10^6) in Matrigel. Five days after injection of cancer cells as tumor xenografts were noted to be growing, the mice were randomly divided into four groups: orally treated with either vehicle [0.6% w/v aqueous Pluronic F-68 (Karyopharm Therapeutics Inc.), $n = 10$], KPT-330 (20 mg/kg, $n = 8$), linsitinib (20 mg/kg, $n = 8$), or KPT-330 plus linsitinib (20 mg/kg each, $n = 8$), thrice weekly × 4 weeks. Mice were given Nutri-Cal (Tomlyn) during experimentation to improve nutrition. Tumor volumes were measured thrice weekly with calipers and were calculated using the following formula: volume (mm^3) = [width (mm)]^2 × length (mm)/2.

Statistical analysis

The mRNA expression levels of CRM1 from various types of primary cancer tissues and cell lines were examined by analyzing Expression Project for Oncology ExpO dataset (URL: https://expo.intgen.org/geo/) and Cancer Cell Line Encyclopedia (CCLE, URL: http://www.broadinstitute.org/ccle; ref. 26), respectively. Combinatorial effects of KPT-330 with linsitinib were examined by MTT, and three-dimensional scatter plots (URL: https://plot.ly/feed/) were used to view drug–drug interactions as previously described (27, 28). The synergism was analyzed by isobologram analysis using the CompuSyn software program (24). All figures from MTT assays are a representative of three replicates. Differences between two groups were analyzed using either paired or unpaired two-tailed Student t test. One-way ANOVA was used for comparisons among multiple groups (*, $P < 0.05$; **, $P < 0.01$). Overlaps of gene lists were identified using online program VENN (URL: http://bioinformatics.psb.ugent.be/webtools/Venn/). Statistical significance of overlapping was determined using χ^2 tests with one degree of freedom and Yates's correction as previously described (29).
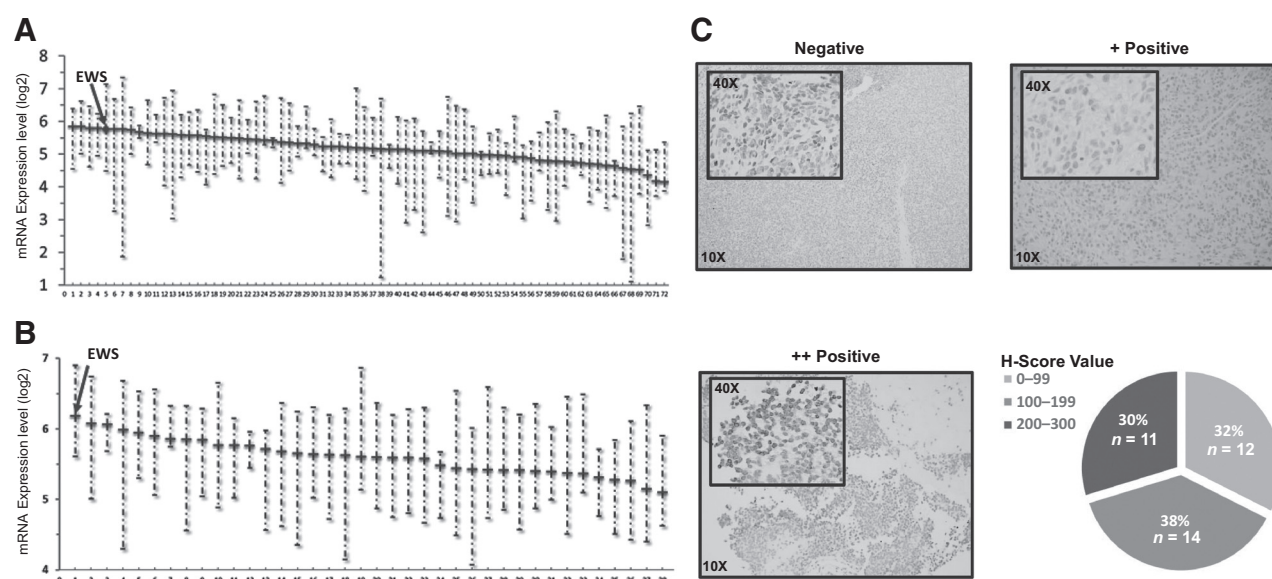
A

B

C

Figure 1.
CRM1 is highly expressed in EWS. A, mRNA level of CRM1 was analyzed from 1,911 primary samples of 72 different cancer types based on Project for Oncology (expO, URL: https://expo.intgen.org/geo/). Tumors with more than three samples were selected. B, mRNA level of CRM1 was analyzed from the CCLE project, which contains data on over 1000 cancer cell lines representing 38 cancer types. Cancer types were shown in Supplementary Table S3. C, representative IHC pictures of CRM1 expression in EWS tissues, with pie charts showing H-scoring.

Results

CRM1 is upregulated in EWS

To evaluate the expression of CRM1 in EWS, we first analyzed 1,911 primary samples from 72 different types of tumors from ExpO (Fig. 1A; Supplementary Table S2). Notably, CRM1 mRNA expression in EWS tumors was the fifth highest among these 72 different cancer types, higher than those tumors that have been shown to have overexpression of CRM1 (11, 13–17). CCLE database analysis also showed that CRM1 mRNA expression in EWS ranked first among 38 different types of cancer cell lines (Fig. 1B; Supplementary Table S3). To determine the expression level of CRM1 protein in EWS, we performed IHC staining on 37 primary EWS tissues and analyzed the staining levels by the H-score method (25). The analysis revealed that 11 samples showed strong nuclear staining (30%, H-score value > 199), 13 samples with moderate nuclear staining (38%, H-score value > 99), and 12 samples showed weak nuclear staining (32%, H-score value 0–99; Fig. 1C; Supplementary Table S4). In addition, CRM1 protein was strongly expressed in all 9 EWS cell lines (Supplementary Fig. S1). These results demonstrated that CRM1 is highly expressed in EWS.
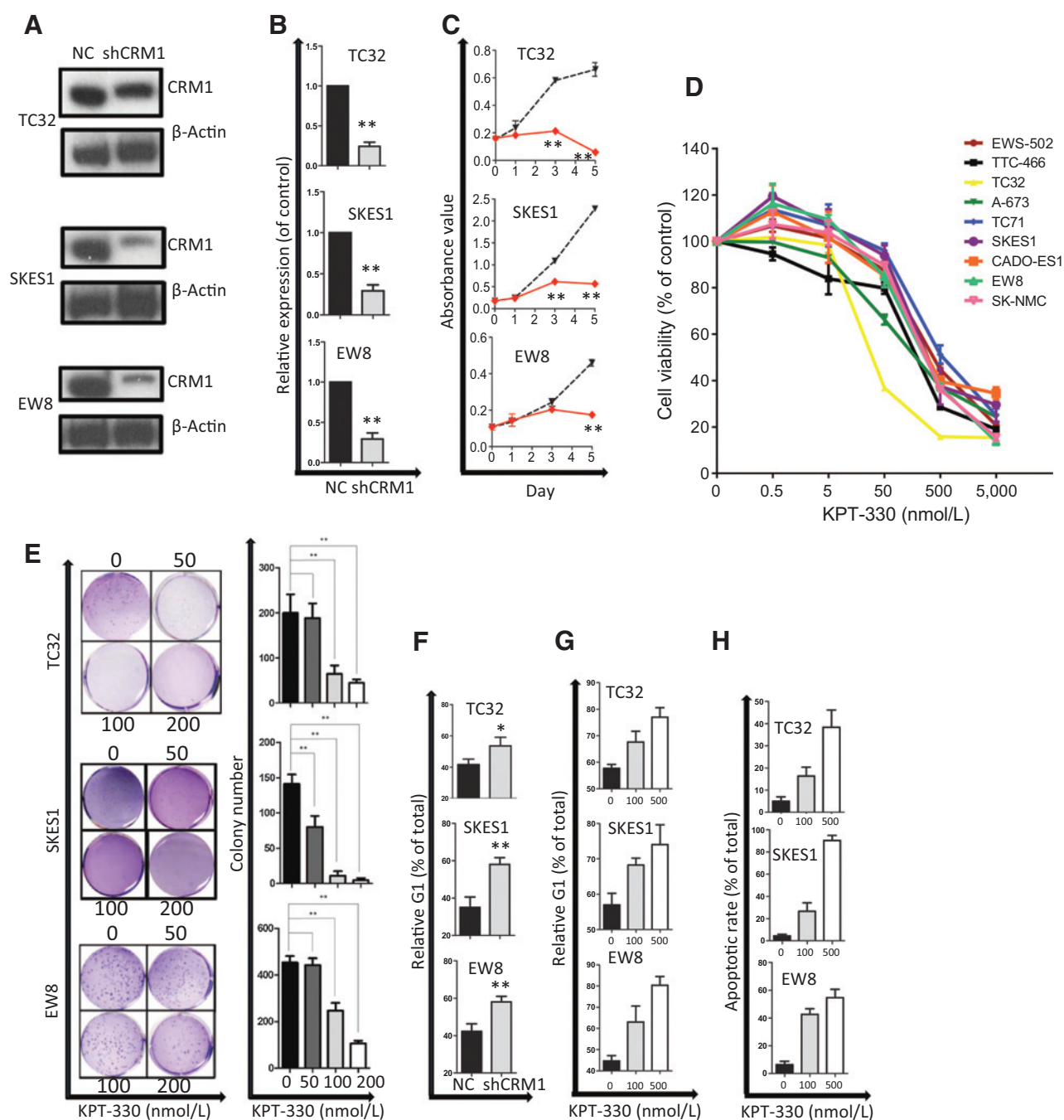
Inhibition of CRM1 decreased cell viability by inducing both apoptosis and G_1 cell-cycle arrest

To determine the biologic significance of CRM1 in EWS, CRM1 was suppressed either by shRNA-mediated knockdown or with the SINE compound KPT-330. Knockdown of CRM1 significantly decreased EWS cell proliferation (Fig. 2A–C), and treatment of KPT-330 dose-dependently inhibited cell viability in all 9 EWS cell lines tested with a mean IC_{50} of approximately 400 nmol/L (Fig. 2D). In addition, KPT-330 markedly inhibited clonogenic growth in EWS cells (Fig. 2E). Moreover, CRM1 inhibition significantly blocked cells in the G_1 phase (Fig. 2F

and G) and induced massive apoptosis (Fig. 2H). In order to test the therapeutic window of KPT-330, we obtained bone marrow samples from three healthy donors, isolated normal $CD34^+$ cells, and measured their dose response to KPT-330 treatment by MTT assay. Results showed a mean IC_{50} of about 9.4 µmol/L (Supplementary Fig. S2), at least 20 times higher than that in EWS cells, suggesting a wide therapeutic window of KPT-330.

Inhibition of CRM1 induced cytotoxicity by repressing EWS-FLI1 and releasing its targeted gene IGFBP3

CRM1 is an important nuclear transporting protein, which regulates the localization of many proteins and mRNAs involved in cell cycle and apoptosis (11, 13–17). To examine downstream targets of CRM1 in EWS, immunoblotting was conducted. Inhibition of CRM1 with shCRM1 or KPT-330 treatment deregulated the expression of several cancer-related proteins, including cyclin D1, p27^{kip1}, p53, p21^{cip1}, and p-MET (Fig. 3A). Notably, CRM1 inhibition (either KPT-330 or shRNA treatment) decreased p53 protein levels in *TP53* wild-type cell lines TC32 and CADO-ES, but not in *TP53*-mutant cell lines (Fig. 3A; Supplementary Fig. S3A). Furthermore, silencing of p53 by siRNA significantly decreased KPT-330–induced apoptosis in TC32 cells (Supplementary Fig. S3B), which was in line with previous findings in *TP53* wild-type leukemic cells (30–34). However, overall no significant correlation occurred between the IC_{50} of EWS cell lines and the mutational status of *TP53* in these cells ($R^2 = 0.27$; $P = 0.15$). Interestingly, EWS-FLI1 was decreased upon CRM1 inhibition (Fig. 3A and B). In contrast, KPT-330 only modestly decreased the level of the fusion protein PAX3-FOXO1 in the rhabdomyosarcoma cell line RH5 and did not affect the expression of FUS-DDIT3 in the myxoid liposarcoma cell line MLS402 (Supplementary Fig. S4).

Figure 2.
Inhibition of CRM1 decreased cell viability by induction of apoptosis and G_1 cell-cycle arrest. A–C, EWS cells were stably infected with either a CRM1-specific shRNA (shCRM1) or scrambled shRNA (NC) control. CRM1 knockdown was evaluated by immunoblotting (A) and qRT-PCR (B). C, cell proliferation was measured by MTT assay. D, cell viability of 9 EWS cell lines, and inhibition of growth was measured by MTT assay. E clonogenic assay of three EWS cell lines. Inhibition of growth was measured by counting colonies using open CFU software (http://opencfu.sourceforge.net/). Right, bar graphs displayed colony numbers in each treatment group. F and G, EWS cells were stably infected with either a shCRM1 or NC control (F), or cells were treated with different concentrations of KPT-330 for 48 hours and stained with PI (G). Bar graphs displayed the proportion of cells in G_1 phase in each treatment group. H, EWS cells were treated with KPT-330 for 24 hours, and Annexin/PI assays were conducted to evaluate the ability of KPT-330 to induce apoptosis. Bar graphs display the percentage of apoptotic cells (positive Annexin V + PI) in each treatment group. Data (B–H) represent mean ± SD, $n = 3$.

We next asked whether EWS-FLI1 was involved in the cell cytotoxicity mediated by CRM1 inhibition. As expected, silencing of EWS-FLI1 through siRNAs decreased EWS cell growth (Fig. 3C and D) and increased the expression of IGFBP3. Notably, silencing of EWS-FLI1 mitigated the growth-inhibitory effects of KPT-330 (Fig. 3E). These results indicated that EWS-FLI1 might be an
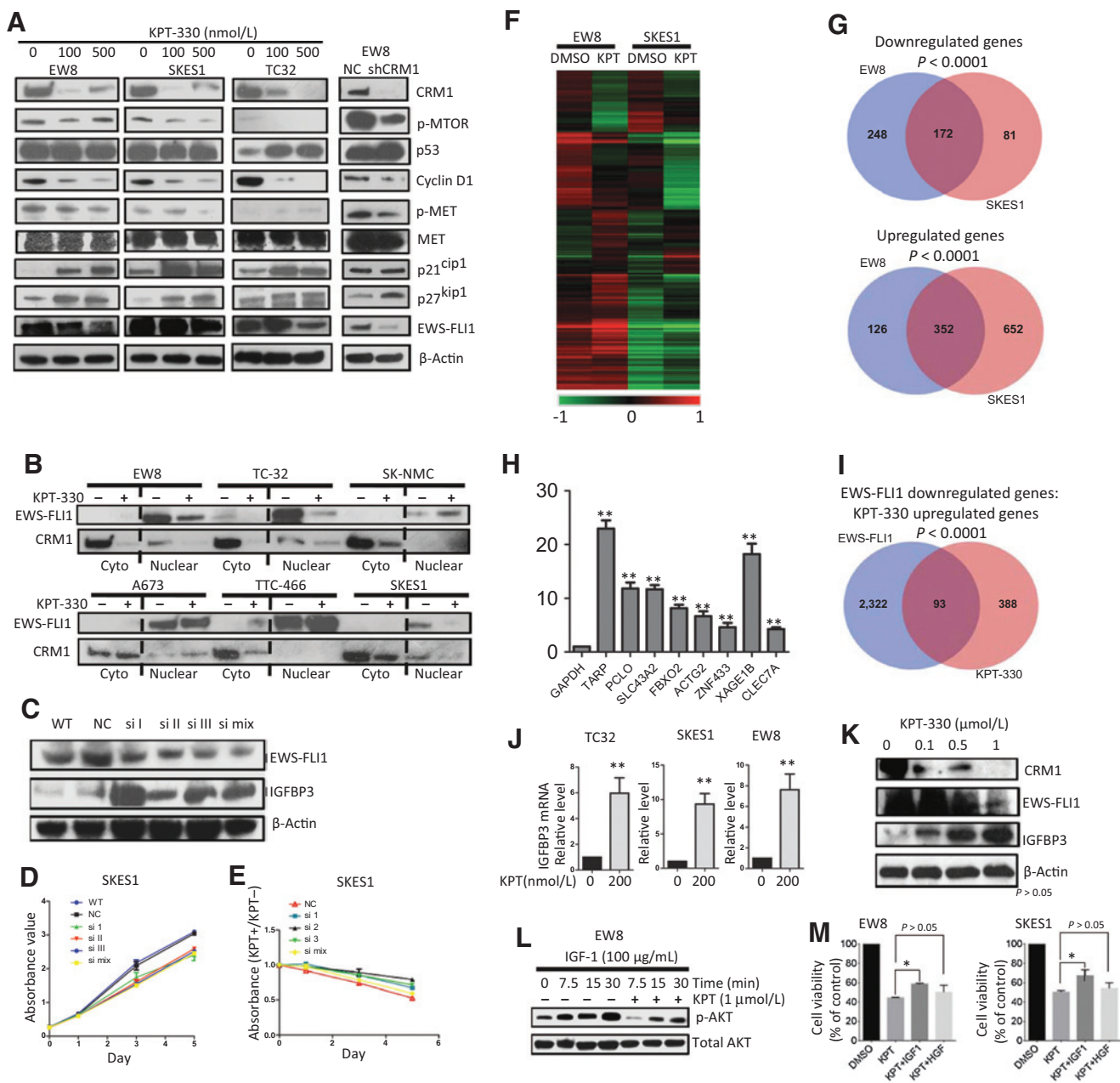
Figure 3.
Inhibition of CRM1 induced cytotoxicity by repressing EWS-FLI1 and its targeted gene IGFBP3. A and B, a panel of EWS cells were treated with either KPT-330, or infected with scramble shRNA (NC) or shRNAs against CRM1 (shCRM1) and subjected to whole-cell lysate immunoblotting (A), or cytoplasmic (Cyto) and nuclear fractionated immunoblotting assays (B) with indicated antibodies. C–E, SKES1 cells were transiently transfected with siRNAs targeting EWS-FLI1 (I, II, III, and mixture of 3) or control siRNA (NC), and subjected to immunoblotting assay with indicated antibodies. D, cell proliferation was measured by MTT assay after 1 to 5 days of culture either with or without exposure to KPT-330 (200 nmol/L). F, heatmap showed alteration of mRNA expression upon KPT-330 treatment of EWS cells. G, Venn diagram of genes regulated by KPT-330 in EW8 cells compared with SKES1 cells. H, EWS cells were exposed to KPT-330 (200 nmol/L), and mRNA level of each gene was evaluated by qRT-PCR. I, Venn diagram of genes codownregulated by KPT-330 compared with genes upregulated by EWS-FLI1. J, IGFBP3 mRNA level was evaluated by qRT-PCR. K, SKES1 cells were exposed to different concentrations of KPT-330, and the proteins were immunoblotted and probed with indicated antibodies. L, EW8 cells were serum starved overnight, treated with KPT-330 (1 μmol/L) for 2 hours, followed by addition of human IGF-1 (100 ng/mL) for indicated durations, and the proteins were immunoblotted and probed with indicated antibodies. M, cells were exposed to different treatment [(KPT-330 (500 nmol/L); KPT-330 (500 nmol/L) + IGF-1 (50 ng/mL); KPT-330 (500 nmol/L) + HGF (50 ng/mL)] for 72 hours, and growth inhibition was measured by MTT assay. Figures are representative of three replicates.

important CRM1-regulated molecule in EWS cells. To screen globally for CRM1-regulated genes in EWS cells, whole-transcriptome sequencing (RNA-seq) was conducted. As shown in Supplementary Table S3 and Fig. 3F and G, 420 (912 transcripts) and 253 (603 transcripts) genes were downregulated ($\log_2 < -0.5$ compared with DMSO group), and 478 (1,089 transcripts) and
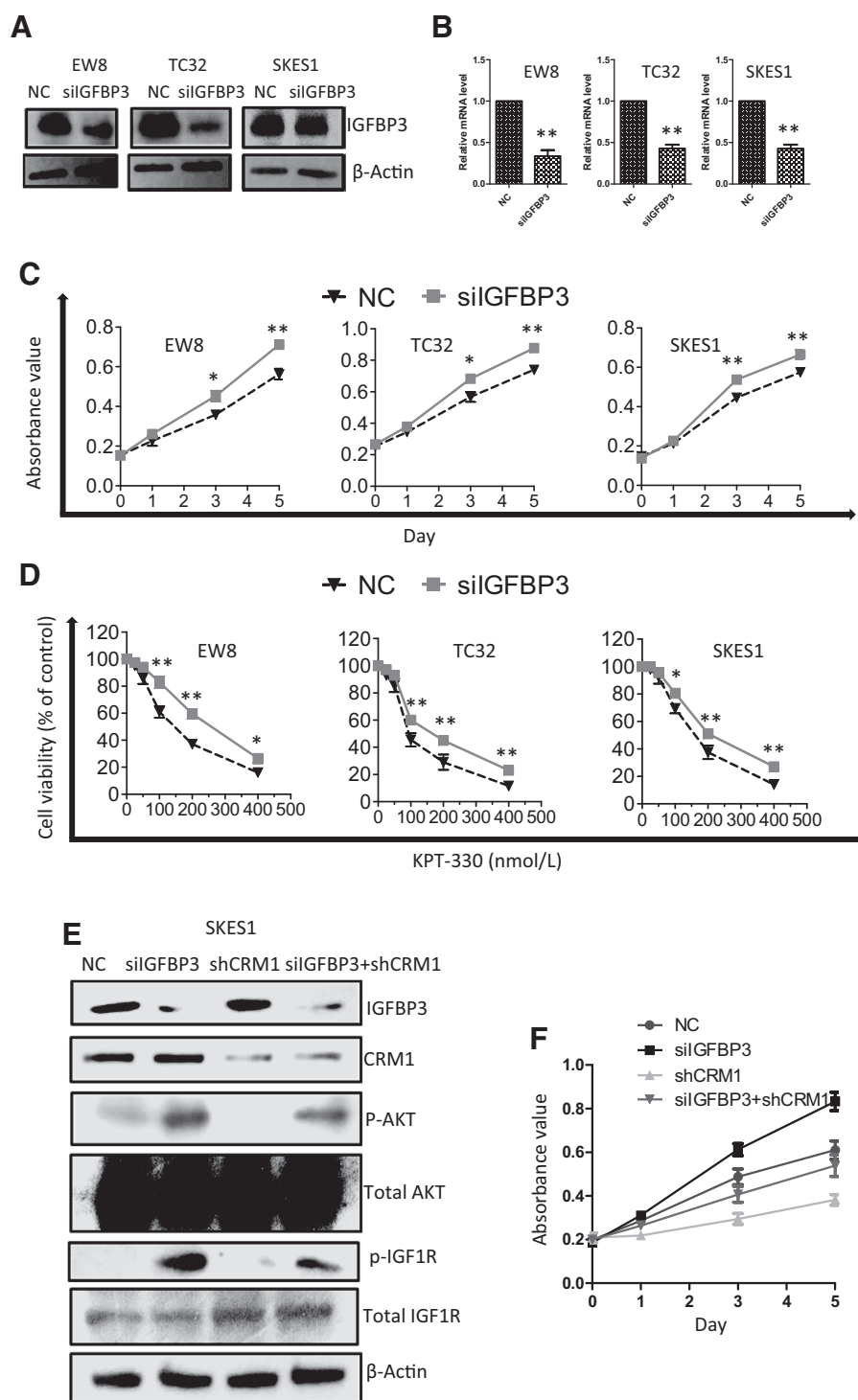
Figure 4.
Knockdown of IGFBP3 rescued inhibitory effect of KPT-330 in EWS cells. A–D, EWS cells were stably infected with either an IGFBP3-specific siRNA (siIGFBP3) or scrambled shRNA (NC) control. IGFBP3 knockdown efficiency was evaluated by immunoblotting (A) and qRT-PCR (B). C, cell proliferation was measured by MTT assay during 1 to 5 days of culture. D, cells were exposed to different concentrations of KPT-330 for 72 hours, and growth inhibition was measured by MTT assay. E and F, SKES1 cells stably expressing indicated shRNAs (NC, siIGFBP3, shCRM1, or siIGFBP3 + shCRM1) were subjected to immunoblotting and probed with indicated antibodies. F, cell proliferation was measured by MTT assay during 1 to 5 days of culture. Figures are representative of three replicates. Data (B, C, D, and F) represent mean $\pm$ SD, $n = 3$.

1,004 (2,201 transcripts) genes were upregulated ($\log_2 > 0.5$ comparing with DMSO group) upon KPT-330 treatment in EW8 and SKES1 cells, respectively. Venn diagram analysis showed that 172 and 352 genes were codownregulated and coupregulated in these two different cell lines, respectively. The co-occurrence of these alterations was statistically significant ($P < 0.00001$, χ^2 tests with one degree of freedom and Yates's correction; Fig. 3G;

Supplementary Table S5). The RNA-seq data were further validated by qRT-PCR through random selection of 9 genes from the coupregulated (6) and codownregulated (3) gene lists (Fig. 3H; Supplementary Table S5). A previous study has shown that knockdown of EWS-FLI1 upregulated 2,415 and downregulated 1,163 genes (9). Strikingly, the overlap of the genes that were coupregulated by KPT-330 in EW8 and SKES1 cells with the genes

that were upregulated by knockdown of EWS-FLI1 was statistically significantly similar ($P < 0.0001$; Fig 3I; Supplementary Table S6). Similarly, the downregulated genes also significantly overlapped ($P < 0.01$; Supplementary Fig. S6; Supplementary Table S6). Notably, many EWS-FLI1–regulated genes, including two IGF-1–binding proteins (IGFBP3 and IGFBP5), were upregulated by either KPT-330 treatment or knockdown of EWS-FLI1 (Fig. 3H; Supplementary Table S5). IGFBP3 is an important EWS-FlLI1 transcriptionally repressed gene, which has been shown to bind and inhibit IGF-1 (35). Constitutive activation of the IGF-1 pathway in EWS was partly attributable to the downregulation of IGFBP3 by EWS-FLI1 (36). The regulation of IGFBP3 by KPT-330 was further confirmed by both qRT-PCR and immunoblotting approaches (Fig. 3J and K). Moreover, we also observed that KPT-330 attenuated AKT activation stimulated by IGF-1 (Fig. 3L), and addition of IGF-1 (50 ng/mL) significantly enhanced cell viability in the presence of KPT-330 (Fig. 3M). In contrast, HGF (50 ng/mL) did not have a rescue effect (Fig. 3M), consistent with its negligible effect on p-AKT activation in EWS cells (data not shown). These results indicated that CRM1 regulated the EWS-FLI1/IGFBP3 pathway, and AKT signaling played a central role in mediating the resistance to both linsitinib and KPT-330 in EWS.

c-MET inhibitor, crizotinib, synergistically enhanced cell killing in combination with KPT-330

As shown in Fig. 3A, CRM1 inhibition also caused downregulation of p-MET expression. c-MET is a receptor tyrosine kinase essential for many cellular actions, and its abnormal activation in cancers, including EWS, correlates with a poor prognosis (37). Targeting c-MET is recognized as a promising opportunity for treatment of human cancers (38, 39). Crizotinib is a c-MET/ALK inhibitor, which has previously been shown to have modest antineoplastic effect against EWS cells *in vitro* (40). In agreement with the prior study, we found crizotinib had a similar inhibitory effect on EWS cell lines, with an IC_{50} about 2 µmol/L (Supplementary Fig. S5A). Notably, combined exposure of both KPT-330 and crizotinib showed synergistic activity against growth of EW8 and SKES1 cells (Supplementary Fig. S5B and S5C). Our results indicate that dual inhibition of c-MET signaling by KPT-330 and crizotinib might be a potential therapeutic option for targeting EWS.

Silencing of IGFBP3 rescued the inhibitory effect of CRM1 inhibition in EWS cells

To examine further the role of IGFBP3 in EWS cells, IGFBP3 was silenced using lentivirus-based siRNA transduction. siIGFBP3 efficiently silenced IGFBP3 (Fig. 4A and B) in EW8, TC32, and SKES1 cells. This caused an increased proliferation of these cells (Fig. 4C). Furthermore, silencing of IGFBP3 increased both p-AKT and p-IGF-1R levels (Fig. 4E). Importantly, knockdown of IGFBP3 partly rescued the inhibitory effect of either KPT-330 treatment (Fig. 4D) or CRM1 knockdown (Fig. 4E and F).

Combination of KPT-330 with linsitinib synergistically inhibited growth of EWS cells

Development of EWS relies on activation of the IGF-1 pathway (35). As an important IGF-1 signaling partner, IGF-1R is recognized as a promising target against this disease (41). Linsitinib (OSI-906) is a potent, orally available small-molecule inhibitor of IGF-1R, which has acceptable tolerability and

preliminary evidence of anti-EWS activity (42, 43). We first determined its IC_{50} for the EWS cell lines *in vitro* (Fig 5A). Inspired by our observations that CRM1 inhibition targeted EWS-FLI1/IGFBP3/IGF-1R signaling, we tested whether CRM1 inhibition and linsitinib might have synergistic anti-EWS effects. Combination of KPT-330 with linsitinib synergistically impaired EWS cell viability in EW8 (mean CI, 0.79), TC32 (mean CI, 0.56), and SKES1 cells (mean CI, 0.44; Fig. 5B). Similarly, shRNA-mediated CRM1 silencing achieved more potent anti-EWS effects when combined with linsitinib, but as expected not when combined with KPT-330 (Fig. 5C, left and middle). Knockdown of IGFBP3 rescued the inhibitory effect of linsitinib in EW8, TC32, and SKES1 cells (Fig. 5C, right). In addition, combination of KPT-330 with linsitinib induced more apoptosis (Fig. 5D) and cell-cycle arrest (Fig. 5E). Moreover, compared with single agent, combination treatment further decreased the expression of progrowth factors, including cyclin D1 and p-AKT, and enhanced the proapoptotic factors, such as BAK, BAX, and IGFBP3 (Fig. 5F).

Combination of KPT-330 with linsitinib significantly inhibited EWS growth *in vivo*

We next examined the anti-EWS property of KPT330 in EW8 (*TP53* mutant) and TC32 (*TP53* wild-type) xenograft models. As shown in Fig. 6, either KPT-330 or linsitinib alone markedly decreased tumor burden compared with vehicle controls in both models (Fig. 6A–F). Importantly, combinational treatment achieved significantly more potent antitumor effects (Fig. 6A–C) in EW8 xenograft model. Consistent with the *in vitro* MTT assay (Fig. 2D), TC32 xenografts were more sensitive to KPT-330 treatment than EW8 *in vivo* (Fig. 6A–F). Due to the dramatic anti-EWS activity mediated by KPT-330 alone, no significant synergistic effect was observed by the combination treatment of the TC32 xenografts (Fig. 6D–F). As shown in Fig. 3L and M, IGFBP3/IGF-1R/p-AKT signaling was regulated by inhibiting CRM1. Therefore, the tumor lysates were examined for expression of p-AKT. Treatment by either KPT-330 alone or in combination with linsitinib robustly decreased the levels of p-AKT (Fig. 6G). We speculate on the mechanisms of synergism with dual inhibition of CRM1 and IGF-1 signaling pathway on Fig. 6H.

Discussion

Until now, more than 240 nuclear proteins have been experimentally confirmed as CRM1-binding cargos (44), many of which are tumor suppressors. Overexpression of CRM1 in cancers causes dysfunction of cell fate regulators and promotes the malignancy of cancer cells. A number of recent studies have shown that targeting CRM1 produces an effective antitumor activity (18–23). Here, by analyzing multiple databases and IHC staining results (Fig. 1), we discovered that CRM1 is highly expressed in EWS, suggesting that it may have important roles in regulation of EWS tumorigenesis.

We observed that inhibition of CRM1 in *TP53* wild-type but not in *TP53*-mutant EWS cell lines resulted in an increased expression of p53. Furthermore, silencing of p53 in TC32 cells (*TP53* wild-type) decreased the activity of apoptosis (Supplementary Fig. S3B). These findings are congruent with the previous findings in *TP53* wild-type leukemic cells (30–34). However, the IC_{50} of EWS cell lines to KPT-330 and the
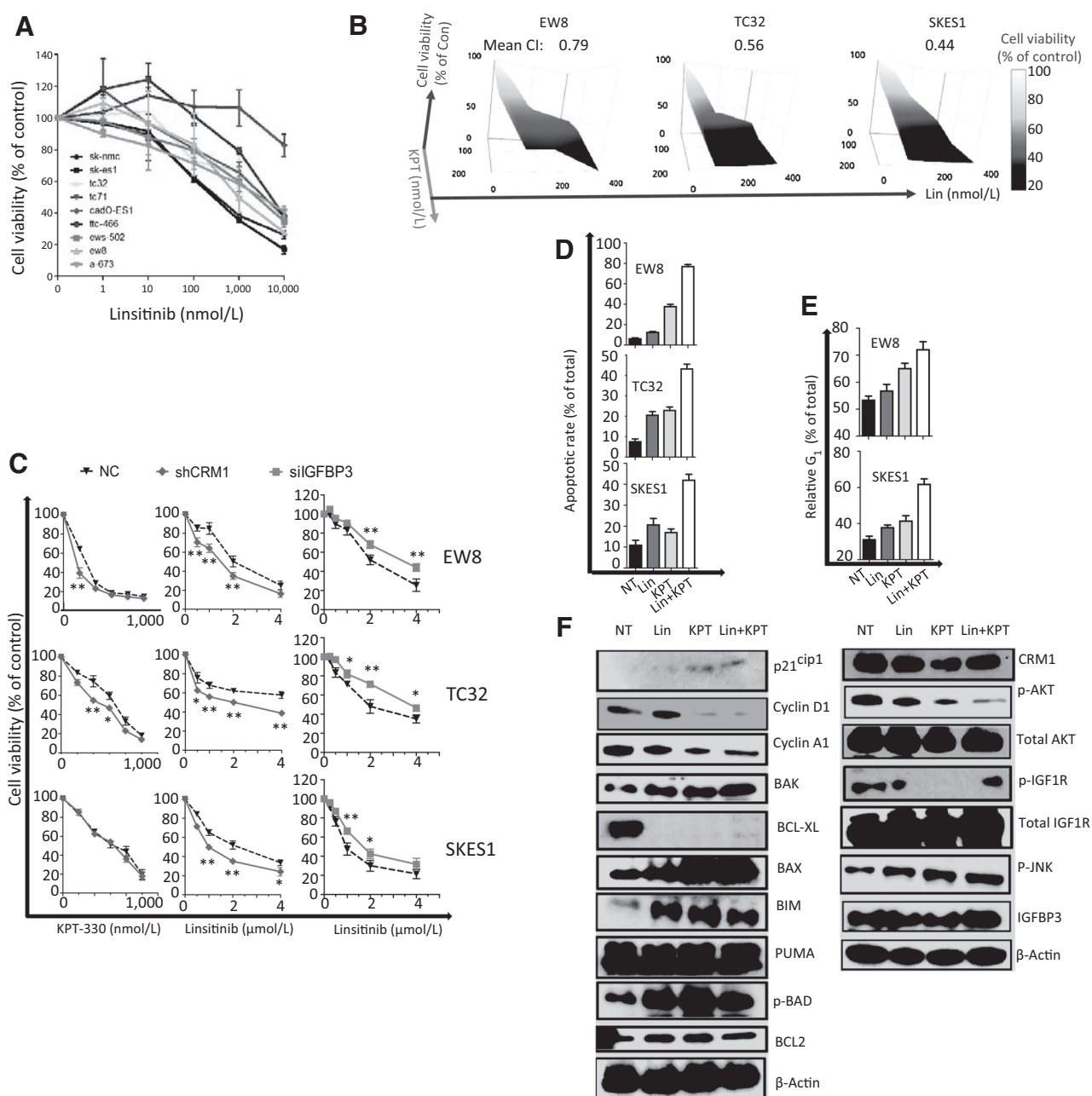
Figure 5.
Combination of KPT-330 with linsitinib synergistically inhibited the growth of EWS cells. A, EWS cells were treated with different concentrations of linsitinb (72 hours), and growth inhibition was measured by MTT assay. B, EWS cells were treated with KPT-330 (0, 50, 100, and 200 nmol/L) and/or linsitinib (0, 100, 200, 400 nmol/L) for 72 hours, and cell viability was measured by MTT assay. Isobologram of the cell survival data was presented by three-dimensional scatter plot, which indicated synergistic cytotoxicity. The color of the isobologram shift from white to black predicted cell viability (100%–20%), which is indicative of synergism. C, EWS cells that were stably expressing either siIGFBP3, shCRM1, or NC control were generated and subjected to MTT assay upon indicated treatment. D–F, EWS cells were treated with linsitinib (Lin, 1 μmol/L), KPT-330 (KPT, 200 nmol/L), or linsitinib (1 μmol/L) + KPT-330 (200 nmol/L; Lin+KPT) for 24 hours, and apoptosis induction (D), cell-cycle progression (E), and protein expression (F) were evaluated. Data (A, C, D, and E) represent mean ± SD, $n = 3$.

mutational status of *TP53* in these cells showed no significant correlation ($R^2 = 0.27$; $P = 0.15$). p53 is an important cargo of CRM1 (45, 46), but clearly for EWS, it is not a biomarker to predict response to KPT-330. This appears to be the same in other studies (18, 19, 47–51). For example, in one of our previous studies, we showed that p73 plays an important role in mediating cell cycle

and apoptosis upon CRM1 inhibition in lung cancer cells with mutant *TP53* (18). Taken together, p53 protein plays an important role in inducing cell apoptosis upon KPT-330 treatment in cancer cells with wild-type *TP53*. But other CRM1 targets such as TP73, IkB, are crucial for mediating KPT-330–dependent cytotoxicity in cancer cells with mutant *TP53*.
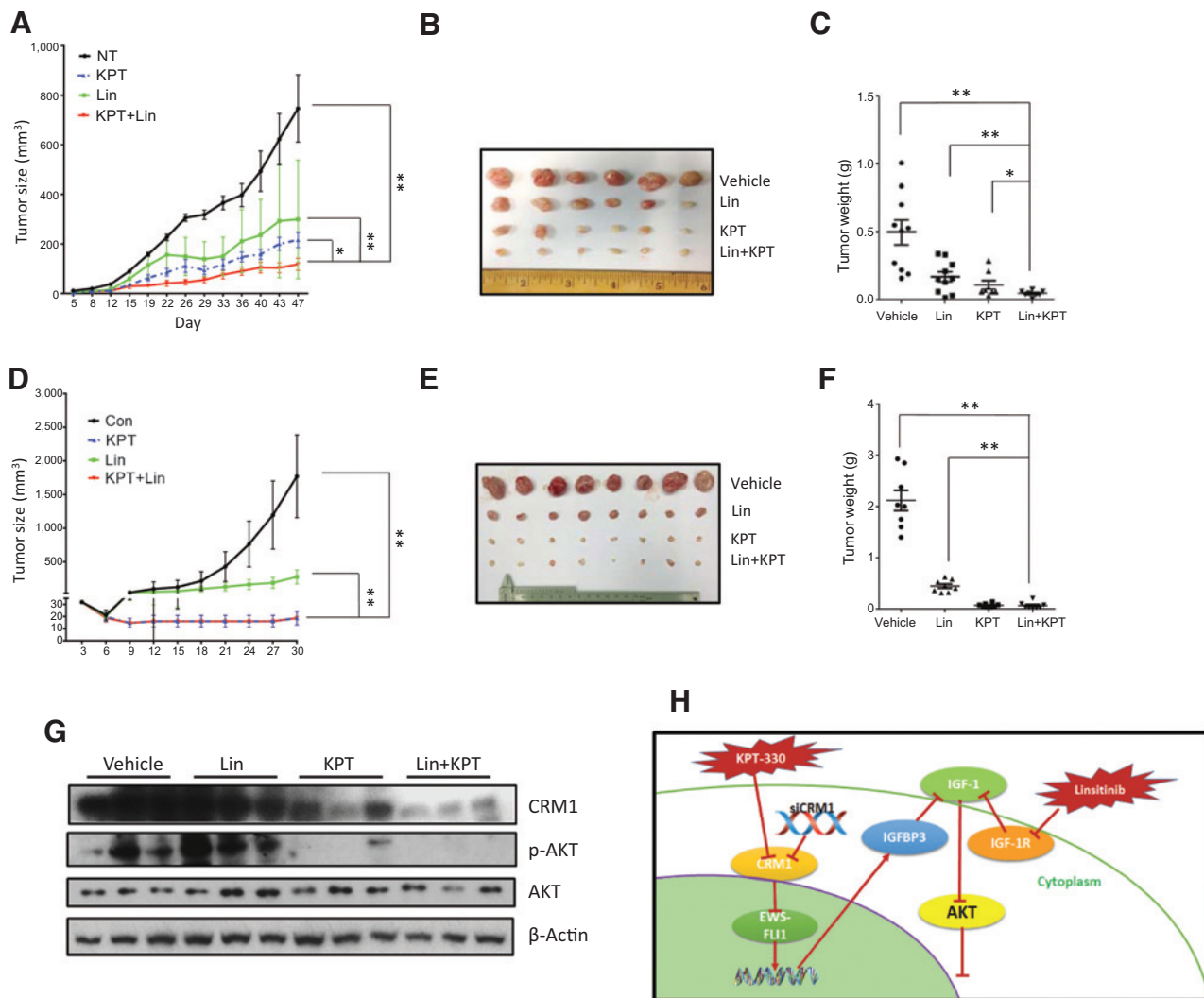
Figure 6.
Combination of KPT-330 with linsitinib synergistically inhibited tumor growth. EW8 and TC32 cells were engrafted in nude mice and treated by gavage with either vehicle, KPT-330 (KPT, 20 mg/kg), linsitinib (Lin, 10 mg/kg), or KPT-330 (20 mg/kg) + linsitinib (20 mg/kg; KPT+Lin). Tumor size during treatment (A and D) and tumor weight at the end point (B, C, E, and F) are shown. G, tumor tissues from EW8 xenografts at the end point were collected, and whole-cell protein was extracted, immunoblotted, and probed with indicated antibodies. H, a cartoon indicates possible molecular mechanisms of synergistic effect between targeting CRM1 and IGF-1R. Data (A, C, D, and F) represent mean $\pm$ SD.

EWS cells have very few somatic mutations highlighting the crucial role of the EWS fusion gene and its downstream pathways in the pathogenesis of the disease (3). Among the numerous EWS-FLI1–regulated genes, IGFBP3 is one of the most extensively investigated. IGFBP3 belongs to the family of IGFBPs. It was originally recognized as an inhibitor of circulating IGFs (52). Beyond its role in transporting IGFs, IGFBP3 is a tumor suppressor, controlling cell proliferation and survival through interacting with pericellular and intracellular compartments (36). In EWS, EWS-FLI1 binds to the IGFBP3 promoter and transcriptionally represses its expression, which in turn enhances IGF-1 signaling (35). In this study, we discovered that EWS-FLI1 is a novel target of CRM1 in several EWS cell lines (TC32, SKES1, and EW8). Either genetic or chemical inhibition of CRM1 suppressed the expression of EWS-FLI1, which released the transcriptional repression of IGFBP3. KPT-330 is the most advanced SINE with >500 cancer patients (hematologic and solid tumors) treated to date in phase I/II clinical trials, and it has been shown to be efficacious in patients with advanced bone and soft tissue sarcoma (unpublished data). Taken together, these results strongly indicate that inhibition of CRM1/EWS-FLI1/IGFBP3 pathway might be a valuable treatment approach for this disease.

Our study showed that CRM1 was highly expressed in all 9 EWS cell lines, and the CRM1 level did not correlate with the sensitivity to KPT-330 treatment ($R^2 = 0.13$; $P = 0.33$). In agreement with our results, several studies have also shown the lack of association between the expression level of CRM1 and the responsiveness to CRM1 inhibitors in different cancer cell lines. For example, Tai and colleagues and Zhang and colleagues found that multiple myeloma cell lines expressed similar levels of CRM1 but varied in their IC_{50}s to KPT inhibitors (50, 51). Therefore, the inhibitory effect of KPT-330 on

different cells might not only depend on the expression level of CRM1, but also rely on its downstream targets.

IGF-1R is a promising target in EWS, and several monoclonal antibodies and chemical inhibitors have been developed (35). Linsitinib (OSI-906) is a potent, selective IGF-1R inhibitor under evaluation in a phase II trial (ORPHA394629) of EWS (42, 43). However, it was found that prolonged treatment of EWS cells with linsitinib *in vivo* caused reactivation of p-AKT (53, 54), which was also observed in our *in vivo* experiments (Fig. 6G). Several studies have shown that an enhanced anticancer effect can be achieved by attacking more than one target in the same pathway by preventing feedback stimulation. For example, Lito and colleagues discovered that RAF inhibitors caused ERK-dependent feedback by reactivation of ligand-dependent signal transduction, and a MEK inhibitor enhanced the antitumor activity of RAF inhibitors (55). Our results demonstrated that dual inhibition of IGF-1 signaling pathway by KPT-330 (which induces IGFBP3) and linsitinib (which represses IGF-1R) achieved superior inhibitory effects both *in vitro* and *in vivo*, providing a potentially promising strategy for the treatment of EWS (Fig. 6H).

Disclosure of Potential Conflicts of Interest

No potential conflicts of interest were disclosed.

Authors' Contributions

Conception and design: H. Sun, D.-C. Lin, H. Marijon, H.P. Koeffler
Development of methodology: H. Sun, D.-C. Lin, H. Marijon, Z. Zhao, J.W. Said
Acquisition of data (provided animals, acquired and managed patients, provided facilities, etc.): H. Sun, Q. Cao, X. Guo, Z. Zhao, L. Xu, B. Pang, V.K.M. Lee, H.J. Lim, N. Doan, J.W. Said, P. Chu, T. Thomas, R. Rajalingam

Analysis and interpretation of data (e.g., statistical analysis, biostatistics, computational analysis): H. Sun, D.-C. Lin, X. Guo, H. Yang, B. Pang, J.W. Said, A. Mayakonda, T. Thomas
Writing, review, and/or revision of the manuscript: H. Sun, D.-C. Lin, S. Gery, J.W. Said, C. Forscher, E. Baloglu, S. Shacham
Administrative, technical, or material support (i.e., reporting or organizing data, constructing databases): H. Sun
Study supervision: D.-C. Lin, H.P. Koeffler

References

1. Castex MP, Rubie H, Stevens MC, Escribano CC, de Gauzy JS, Gomez-Brouchet A, et al. Extraosseous localized Ewing tumors: improved outcome with anthracyclines–French society of pediatric oncology and international society of pediatric oncology. J Clin Oncol 2007;25:1176–82.
2. Dantonello TM, Int-Veen C, Harms D, Leuschner I, Schmidt BF, Herbst M, et al. Cooperative trial CWS-91 for localized soft tissue sarcoma in children, adolescents, and young adults. J Clin Oncol 2009;27:1446–55.
3. Balamuth NJ, Womer RB. Ewing's sarcoma. Lancet Oncol 2010;11:184–92.
4. Tirode F, Surdez D, Ma X, Parker M, Le Deley MC, Bahrami A, et al. Genomic landscape of Ewing sarcoma defines an aggressive subtype with co-association of STAG2 and TP53 mutations. Cancer Discov 2014;4:1342–53.
5. Riggi N, Stamenkovic I. The Biology of Ewing sarcoma. Cancer Lett 2007;254:1–10.
6. Brohl AS, Solomon DA, Chang W, Wang J, Song Y, Sindiri S, et al. The genomic landscape of the Ewing sarcoma family of tumors reveals recurrent STAG2 mutation. PLoS Genetics 2014;10:e1004475.
7. Crompton BD, Stewart C, Taylor-Weiner A, Alexe G, Kurek KC, Calicchio ML, et al. The genomic landscape of pediatric Ewing sarcoma. Cancer Discov 2014;4:1326–41.
8. Riggi N, Knoechel B, Gillespie SM, Rheinbay E, Boulay G, Suva ML, et al. EWS-FLI1 utilizes divergent chromatin remodeling mechanisms to directly activate or repress enhancer elements in Ewing sarcoma. Cancer Cell 2014;26:668–81.
9. Smith R, Owen LA, Trem DJ, Wong JS, Whangbo JS, Golub TR, et al. Expression profiling of EWS/FLI identifies NKX2.2 as a critical target gene in Ewing's sarcoma. Cancer Cell 2006;9:405–16.
10. Hutten S, Kehlenbach RH. CRM1-mediated nuclear export: To the pore and beyond. Trends Cell Biol 2007;17:193–201.
11. Turner JG, Sullivan DM. CRM1-mediated nuclear export of proteins and drug resistance in cancer. Curr Med Chem 2008;15:2648–55.
12. Nguyen KT, Holloway MP, Altura RA. The CRM1 nuclear export protein in normal development and disease. Int J Biochem Mol Biol 2012;3:137–51.
13. Zhou F, Qiu W, Yao R, Xiang J, Sun X, Liu S, et al. CRM1 is a novel independent prognostic factor for the poor prognosis of gastric carcinomas. Medical Oncol 2013;30:726.
14. Kutay U, Hetzer MW. Reorganization of the nuclear envelope during open mitosis. Curr Opinion Cell Biol 2008;20:669–77.
15. Kojima K, Kornblau SM, Ruvolo V, Dilip A, Duvvuri S, Davis RE, et al. Prognostic impact and targeting of CRM1 in acute myeloid leukemia. Blood 2013;121:4166–74.
16. Huang WY, Yue L, Qiu WS, Wang LW, Zhou XH, Sun YJ. Prognostic value of CRM1 in pancreas cancer. Clin Invest Med 2009;32:E315.
17. Shen A, Wang Y, Zhao Y, Zou L, Sun L, Cheng C. Expression of CRM1 in human gliomas and its significance in p27 expression and clinical prognosis. Neurosurgery 2009;65:153–9; discussion 59–60.
18. Sun H, Hattori N, Chien W, Sun Q, Sudo M, GL EL, et al. KPT-330 has antitumour activity against non-small cell lung cancer. Br J Cancer 2014;111:281–91.
19. Zheng Y, Gery S, Sun H, Shacham S, Kauffman M, Koeffler HP. KPT-330 inhibitor of XPO1-mediated nuclear export has anti-proliferative activity in hepatocellular carcinoma. Cancer Chemother Pharmacol 2014;74:487–95.
20. Lapalombella R, Sun Q, Williams K, Tangeman L, Jha S, Zhong Y, et al. Selective inhibitors of nuclear export show that CRM1/XPO1 is a target in chronic lymphocytic leukemia. Blood 2012;120:4621–34.
21. Ranganathan P, Yu X, Na C, Santhanam R, Shacham S, Kauffman M, et al. Preclinical activity of a novel CRM1 inhibitor in acute myeloid leukemia. Blood 2012;120:1765–73.
22. Walker CJ, Oaks JJ, Santhanam R, Neviani P, Harb JG, Ferenchak G, et al. Preclinical and clinical efficacy of XPO1/CRM1 inhibition by the karyopherin inhibitor KPT-330 in Ph+ leukemias. Blood 2013;122:3034–44.
23. Schmidt J, Braggio E, Kortuem KM, Egan JB, Zhu YX, Xin CS, et al. Genome-wide studies in multiple myeloma identify XPO1/CRM1 as a critical target validated using the selective nuclear export inhibitor KPT-276. Leukemia 2013;27:2357–65.

24. Chou TC. Drug combination studies and their synergy quantification using the Chou-Talalay method. Cancer Res 2010;70:440–6.
25. McCarty KSJr., Miller LS, Cox EB, Konrath J, McCarty KSSr. Estrogen receptor analyses. Correlation of biochemical and immunohistochemical methods using monoclonal antireceptor antibodies. Arch Pathol Lab Med 1985;109:716–21.
26. Barretina J, Caponigro G, Stransky N, Venkatesan K, Margolin AA, Kim S, et al. The Cancer Cell Line Encyclopedia enables predictive modelling of anticancer drug sensitivity. Nature 2012;483:603–7.
27. Zhao W, Yang H. Statistical methods in drug combination studies. New York: Chapman and Hall/CRC; 2014.
28. Suhnel J. Comment on the paper: A three-dimensional model to analyze drug-drug interactions. Prichard, M.N. and Shipman, C., Jr. (1990) Anti-viral Res. 14, 181–206. Antiviral Res 1992;17:91–8.
29. Ihara M, Meyer-Ficca ML, Leu NA, Rao S, Li F, Gregory BD, et al. Paternal poly (ADP-ribose) metabolism modulates retention of inheritable sperm histones and early embryonic gene expression. PLoS Genetics 2014;10: e1004317.
30. Zhao Z, Zuber J, Diaz-Flores E, Lintault L, Kogan SC, Shannon K, et al. p53 loss promotes acute myeloid leukemia by enabling aberrant self-renewal. Genes Dev 2010;24:1389–402.
31. Cheng J, Yee JK, Yeargin J, Friedmann T, Haas M. Suppression of acute lymphoblastic leukemia by the human wild-type p53 gene. Cancer Res 1992;52:222–6.
32. Xu J, Timares L, Heilpern C, Weng Z, Li C, Xu H, et al. Targeting wild-type and mutant p53 with small molecule CP-31398 blocks the growth of rhabdomyosarcoma by inducing reactive oxygen species-dependent apoptosis. Cancer Res 2010;70:6566–76.
33. Lanza F, Bi S. Role of p53 in leukemogenesis of chronic myeloid leukemia. Stem Cells 1995;13:445–52.
34. Yeargin J, Cheng J, Haas M. Role of the p53 tumor suppressor gene in the pathogenesis and in the suppression of acute lymphoblastic T-cell leukemia. Leukemia 1992;6 Suppl3:85S–91S.
35. Ho AL, Schwartz GK. Targeting of insulin-like growth factor type 1 receptor in Ewing sarcoma: Unfulfilled promise or a promising beginning? J Clin Oncol 2011;29:4581–3.
36. Holly J. IGF-1, IGFBP-3, and cancer risk. Lancet 2004;364:325–6; author reply 26-7.
37. Organ SL, Tsao MS. An overview of the c-MET signaling pathway. Ther Adv Med Oncol 2011;3:S7–S19.
38. Liu X, Newton RC, Scherle PA. Developing c-MET pathway inhibitors for cancer therapy: Progress and challenges. Trends Mol Med 2010;16:37–45.
39. Davis IJ, McFadden AW, Zhang Y, Coxon A, Burgess TL, Wagner AJ, et al. Identification of the receptor tyrosine kinase c-Met and its ligand, hepatocyte growth factor, as therapeutic targets in clear cell sarcoma. Cancer Res 2010;70:639–45.
40. Fleuren ED, Roeffen MH, Leenders WP, Flucke UE, Vlenterie M, Schreuder HW, et al. Expression and clinical relevance of MET and ALK in Ewing sarcomas. Int J Cancer 2013;133:427–36.
41. Toretsky JA, Gorlick R. IGF-1R targeted treatment of sarcoma. Lancet Oncol 2010;11:105–6.
42. Fassnacht M, Berruti A, Baudin E, Demeure MJ, Gilbert J, Haak H, et al. Linsitinib (OSI-906) versus placebo for patients with locally advanced or metastatic adrenocortical carcinoma: a double-blind, randomised, phase 3 study. Lancet Oncol 2015;16:426–35.
43. Bendell JC, Jones SF, Hart L, Spigel DR, Lane CM, Earwood C, et al. A phase Ib study of linsitinib (OSI-906), a dual inhibitor of IGF-1R and IR tyrosine kinase, in combination with everolimus as treatment for patients with refractory metastatic colorectal cancer. Invest New Drugs 2015;33:187–93.
44. Xu D, Grishin NV, Chook YM. NESdb: A database of NES-containing CRM1 cargoes. Mol Biol Cell 2012;23:3673–6.
45. Kanai M, Hanashiro K, Kim SH, Hanai S, Boulares AH, Miwa M, et al. Inhibition of Crm1-p53 interaction and nuclear export of p53 by poly (ADP-ribosyl)ation. Nat Cell Biol 2007;9:1175–83.
46. Dickmanns A, Monecke T, Ficner R. Structural basis of targeting the exportin CRM1 in cancer. Cells 2015;4:538–68.
47. De Cesare M, Cominetti D, Doldi V, Lopergolo A, Deraco M, Gandellini P, et al. Anti-tumor activity of selective inhibitors of XPO1/CRM1-mediated nuclear export in diffuse malignant peritoneal mesothelioma: the role of survivin. Oncotarget 2015;6:13119–32.
48. Etchin J, Sanda T, Mansour MR, Kentsis A, Montero J, Le BT, et al. KPT-330 inhibitor of CRM1 (XPO1)-mediated nuclear export has selective anti-leukaemic activity in preclinical models of T-cell acute lymphoblastic leukaemia and acute myeloid leukaemia. Br J Haematol 2013; 161:117–27.
49. Cheng Y, Holloway MP, Nguyen K, McCauley D, Landesman Y, Kauffman MG, et al. XPO1 (CRM1) inhibition represses STAT3 activation to drive a survivin-dependent oncogenic switch in triple-negative breast cancer. Mol Cancer Therapeutics 2014;13:675–86.
50. Tai YT, Landesman Y, Acharya C, Calle Y, Zhong MY, Cea M, et al. CRM1 inhibition induces tumor cell cytotoxicity and impairs osteoclastogenesis in multiple myeloma: molecular mechanisms and therapeutic implications. Leukemia 2014;28:155–65.
51. Zhang K, Wang M, Tamayo AT, Shacham S, Kauffman M, Lee J, et al. Novel selective inhibitors of nuclear export CRM1 antagonists for therapy in mantle cell lymphoma. Exp Hematol 2013;41:67–78 e4.
52. Martin JL, Baxter RC. Signalling pathways of insulin-like growth factors (IGFs) and IGF binding protein-3. Growth factors 2011;29:235–44.
53. Knight T, Irving JA. Ras/Raf/MEK/ERK pathway activation in childhood acute lymphoblastic leukemia and its therapeutic targeting. Frontiers in oncology 2014;4:160.
54. Jahangiri A, Weiss WA. It takes two to tango: Dual inhibition of PI3K and MAPK in rhabdomyosarcoma. Clin Cancer Res 2013;19:5811–3.
55. Lito P, Pratilas CA, Joseph EW, Tadi M, Halilovic E, Zubrowski M, et al. Relief of profound feedback inhibition of mitogenic signaling by RAF inhibitors attenuates their activity in BRAFV600E melanomas. Cancer Cell 2012;22:668–82.